GEOLOGY OF SATURN'S SATELLITE RHEA ON THE BASIS OF THE HIGH-RESOLUTION IMAGES FROM THE TARGETED FLYBY 049 ON AUG. 30, 2007. R. J. Wagner[1], G. Neukum[2], B. Giese[1], T. Roatsch[1], T. Denk[2], U. Wolf[2], and C. C. Porco[3]. [1]Inst. of Planetary Research, German Aerospace Center (DLR), Rutherford-strasse 2, D-12489 Berlin, Germany, e-mail: roland.wagner@dlr.de; [2]Inst. of Geosciences, Freie Universitaet Berlin (FUB), D-12249 Berlin, Germany; [3]Space Science Institute, Boulder, CO., USA.

Introduction: Rhea is Saturn's second-largest satellite (1528 km diameter). The low average density of 1.233 gcm^{-3} [1] implies a more or less icy body. The high geometric albedo (0.65) and the presence of H_2O absorption bands imply that water ice is also the dominant surface constituent [e.g. 2]. During a close flyby of the Cassini spacecraft at Rhea, the axial moment of inertia could be determined which showed that this satellite is more or less a homogeneous, not differentiated body composed of approximately 75% ice and 25% rock and metal [3].

Geology of Rhea prior to Cassini: At a maximum spatial resolution of 500 m/pxl, Rhea was the best one imaged of the saturnian moons. Voyager-1 images showed a densely cratered leading hemisphere, while the trailing hemisphere, seen only at very low resolution, was characterized by bright, filament-like wispy markings, similar to those on Rhea's inner neighbor Dione [4]. The densely cratered terrain, including ring structures, was subdivided into several units by different investigators, based on crater abundance, texture, and the presence of lineations [5][6]. Tectonic features are troughs, scarps, ridges (of minor abundance), and lineaments [5][6][7]. As for Dione, Cassini ISS data revealed that the bright wispy markings represent tectonic features [8].

Cassini ISS image data base. Rhea was imaged by the Cassini Narrow Angle (NAC) and Wide Angle Camera (WAC) [9] during several non-targeted flybys at resolutions better than 1 km/pxl (in flybys 00C, 005, 016, 018 - 020, 022, 027). The targeted flyby 049 on August 30, 2007, provided extensive areal coverage and high-resolution imaging of the densely cratered plains, basins, and of a bright ray crater, primarily in the leading hemisphere.

Methodology: The work presented in this paper continues our comparative investigations of Rhea's inner neighbor Dione [8]. (1) The units are mapped, based on albedo and morphology. (2) Ages of these units are obtained from *crater size-frequency measurements* and from application of *impact chronology models*. Absolute ages are assigned by means of impact cratering chronology models: (a) *Model I*, based on a lunar-like cratering rate, preferentially by asteroids [10][11][12], and (b) *Model II* with a constant cratering rate, primarily by comets [13].

Results: At regional scale (300 -1000 m/pxl), the densely cratered plains on Rhea show little variation in terms of albedo and morphology. In spite of the high density of craters, measured crater frequencies in flyby 049 data are production distributions similar to lunar crater distributions, confirming previous results using ISS camera data [8] (*Fig. 1*). Average cratering model ages in the cratered plains are on the order of 4.2 Gyr (*Model I*, [12]) or 3.6 Gyr (*Model II*, [13]). Some variations in large-crater abundances discussed by [5][6][14] can be confirmed. Smoother areas with a paucity of smaller craters are also observed but lack clear evidence for cryovolcanic resurfacing, or mantling by airfall deposits as discussed by [6]. Based on Rhea's more or less undifferentiated state [3] it seems unlikely that cryovolcanic activity has ever occured, however.

Basins and large craters. Large craters and basins are abundant, but are heavily degraded and are more easily detected and mapped using digital terrain models. The anti-Saturnian hemisphere is characterized by two well-preserved basins, 400 to 500 km in diameter. While a lower crater density and hence a younger age was reported for the Tirawa basin [5], our crater counts show that crater frequencies inside Tirawa and the adjacent (unnamed) basin are comparable to the frequencies outside, therefore both basins are also rather old features on the order of 4 Gyr.

Bright ray crater. While stratigraphically young, bright ray craters characterize the surfaces of the icy satellites of Jupiter, they are not common on the saturnian satellites [8, and refs. therein]. Only one prominent ray crater is found on Rhea, located at lat. 12.5° S, long. 112° W. The bright rays of the 48-km crater show a butterfly wing pattern implying an oblique impact from the west. The flyby 049 images reveal that the frequency of small craters on the ray crater floor and in the continuous ejecta blanket is very low, inferring the crater is rather young. This is confirmed by the cratering model ages, measured in the continuous ejecta blanket, which are on the order of ~ 280 Myr and ~ 8 Myr (*Model I* and *II*, respectively). Secondary chains and bright rays extend several hundreds of kilometers outward. One intriguing feature is the occurrence of small clusters, resembling small secondaries, within the crater floor and in the continuous

ejecta. Since there is no crater younger than the ray crater at close range as a possible source, two explanations remain: (1) the small clusters were created by material ejected at a steep angle which re-impacted a part of the crater floor and continuous ejecta [15]. (2) More likely, the crater clusters originate from material disintegrated from the major projectile which impacted upon the formation of the larger primary crater.

References: [1] Thomas P. C. et al. (2006), *LPSC XXXVII,* abstr. No. 1639. [2] Clark R. N. et al. (1986), in *Saturn*, UofA Press, Tucson, Az., p. 437-491. [3] Schubert G., et al., *AGU Fall Meeting Abstr.*, D6, 2006. [4] Smith et al. (1981), *Science 212,* 163-191. [5] Moore J. M. et al. (1985), *JGR 90 (suppl.),* C785-C795. [6] Plescia J. B. (1985), *NASA-TM 87563*, 585-587. [7] Thomas P. G. (1987), *Icarus 74*, 554-567. [8] Wagner R. et al. (2006), *LPSC XXXVII*, abstr. No. 1805. [9] Porco C. C. et al., *SSR 115*, 363-497, 2004. [10] Boyce J. & Plescia J. (1985), in: *Ices in the Solar System* (D. Reidel Publ.), p. 791-804. [11] Neukum G. (1985), *Adv. Space Res*. 5, 107-116. [12] Neukum G. et al. (2005), *LPSC XXXVI*, abstr. No. 2034. [13] Zahnle K. et al. (2003), *Icarus 163*, 263-289. [14] Lissauer J. J. et al. (1988), *JGR 96*, No. B11, 13,776 – 13,804. [15] Greeley R. et al., *Satellites of Jupiter*, (D. Morrison, ed.) UofA Press Tucson, Az., 340-378, 1982.

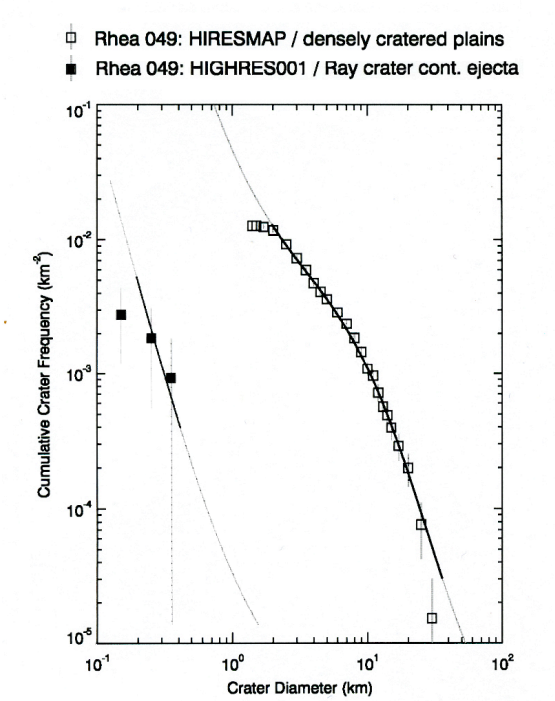

Fig. 1: Cumulative crater size-frequency distribution measured on ISS data from flyby 049 (WAC frame W1567129584, 380 m/pxl) (open quadrangles). Curve shown is the lunar highland curve, adjusted to impact conditions on Rhea. Closed quadrangles from ejecta blanket of the bright ray crater (see *Fig. 2*) (observation: HIGHRES001; ca. 40 m/pxl resolution).

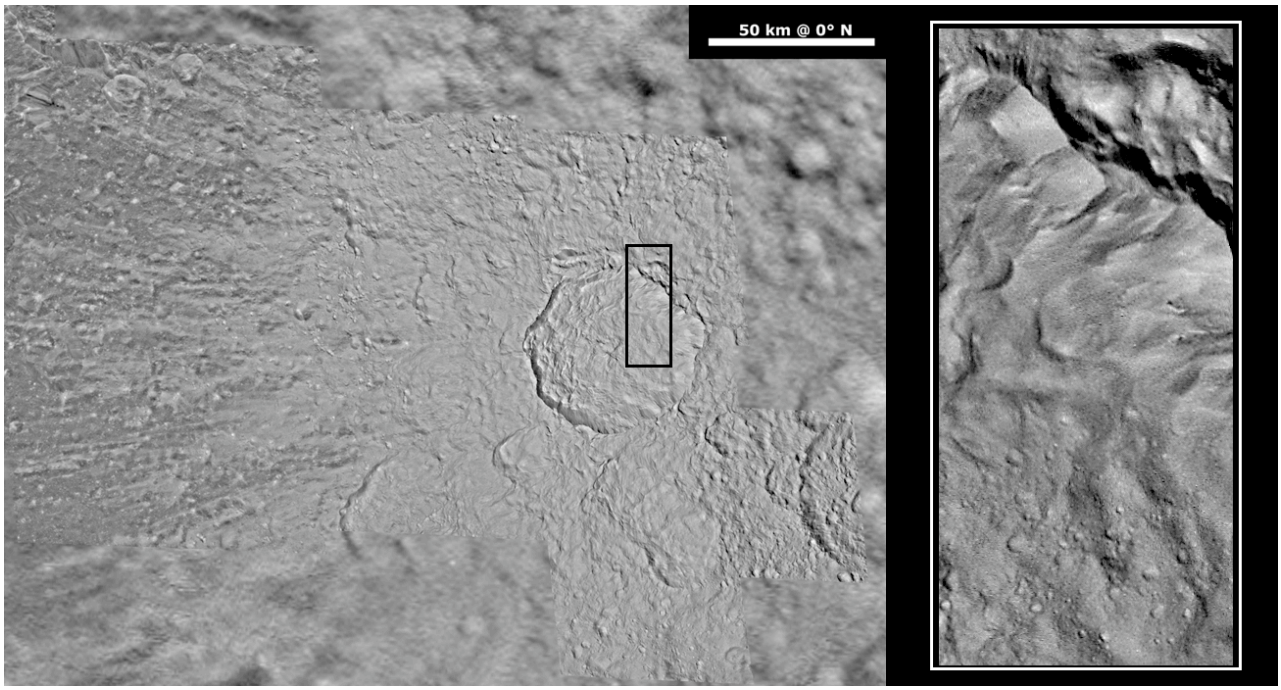

Fig. 2: *Left* – Mosaic of NAC frames from flyby 049 ISS data (observation HIGHRES001) showing the bright ray crater at ~ 40 m/pxl in WAC context. *Right* - detail of crater floor and rim with "secondaries" on crater floor.